

important one, since the thickness of most industrially processed polymer films (blown or drawn) is too great to allow transmission IR dichroism studies to probe bulk average characteristics. Comparing with the trirefringence technique,²¹ where three spatial refractive indices can be measured by modifying an Abbe-type refractometer to estimate orientation, our IR ATR dichroism technique provides more detailed information on surface structure and orientation as demonstrated in this study.

Future Studies. For a surface depth greater than 10 μm , FT IR photoacoustic spectroscopy with a polarized IR beam was found useful to assess orientation.²² A combination of FT IR ATR and photoacoustic dichroism studies will thus permit the probing of the surface structure and orientation as a function of a wider range of depths. For surface characterization in the range of a few thousand angstroms, a denser crystal such as Ge can be used. If one wants to limit the probing to hundreds of angstroms, a combination of a even denser crystal with a very high incidence angle should be used with longer scanning and improved optics (e.g., better focusing of the IR signal by a beam condenser).

Also, three-dimensional surface molecular orientation characterization in such polymers as liquid crystalline polymers, piezoelectric polymers, or chemically modified surfaces and correlating with surface-dependent properties will be interesting applications for this technique. We plan to continue our future studies in these directions.

Acknowledgment. This work was in part supported by the Office of Naval Research. We acknowledge the generosity of Digilab for access to an FTS-15 Fourier transform infrared spectrometer. We are grateful for the samples and interests of Dr. de Vries and Dr. Willis and to Prof. Seferis for providing biaxially oriented samples

and their refractive index values. Thanks are also due Prof. N. H. Sung for help with the manuscript.

Registry No. Polypropylene, 9003-07-0; poly(ethylene terephthalate), 25038-59-9.

References and Notes

- (1) Flournoy, P. A.; Schaeffers, W. J. *Spectrochim. Acta* 1966, 22, 5.
- (2) Hansen, W. H. *Spectrochim. Acta* 1965, 21, 815.
- (3) Sung, C. S. P. *Macromolecules* 1981, 14, 591.
- (4) Garton, A.; Carlsson, D. J.; Wiles, D. M. *Appl. Spectrosc.* 1981, 35, 432.
- (5) Schmidt, P. G. *J. Polym. Sci., Part A* 1963, 1, 1271.
- (6) Jasse, B.; Koenig, J. L. *J. Macromol. Sci., Rev. Macromol. Chem.* 1979, C17, 61.
- (7) de Vries, A. *J. Pure Appl. Chem.* 1981, 53, 1011.
- (8) Harrick, N. J. "Internal Reflection Spectroscopy", 2nd ed.; Harrick Scientific Corp.: Ossining, NY, 1979.
- (9) Samuels, R. J. "Structured Polymer Properties"; Wiley-Interscience: New York, 1974.
- (10) Hutchinson, I. J.; Ward, I. M.; Willis, H. A.; Zichy, V. *Polymer* 1980, 21, 55.
- (11) Quynn, R. G.; Riley, J. L.; Young, D. A.; Noether, H. D. *J. Appl. Polym. Sci.* 1959, 2, 166.
- (12) Krimm, S. *Fortschr. Hochpolym. Forsch.* 1960, 2, 51.
- (13) Zerbi, G.; Pisen, L. *J. Chem. Phys.* 1968, 49, 3840.
- (14) Jarvis, D. A.; Hutchinson, I. J.; Bower, D. I.; Ward, I. M. *Polymer* 1980, 21, 41.
- (15) Cunningham, A.; Ward, I. M.; Willis, H. A.; Zichy, V. *Polymer* 1974, 15, 749.
- (16) Grime, D.; Ward, I. M. *Trans. Faraday Soc.* 1958, 54, 959.
- (17) Farrow, G.; Ward, I. M. *Polymer* 1960, 1, 330.
- (18) Koenig, J. L.; Cornell, S. W. *J. Polym. Sci., Part C* 1969, 22, 1019.
- (19) de Vries, A. *J. Pure Appl. Chem.* 1982, 54, 647.
- (20) Desper, C. R. "Characterization of Materials in Research, Ceramics and Polymers"; Syracuse University Press: Syracuse, NY, 1975.
- (21) Samuels, R. J. *J. Appl. Polym. Sci.* 1981, 26, 1383.
- (22) Krishnan, K.; Hill, S.; Hobbs, J. P.; Sung, C. S. P. *Appl. Spectrosc.* 1982, 36, 257.

Structural Studies of Poly(ethylenimine). 3. Structural Characterization of Anhydrous and Hydrated States and Crystal Structure of the Hemihydrate

Yozo Chatani,* Takushi Kobatake, and Hiroyuki Tadokoro

Department of Macromolecular Science, Faculty of Science, Osaka University, Toyonaka, Osaka 560, Japan. Received May 21, 1982

ABSTRACT: A series of X-ray studies on the absorption of water vapor by poly(ethylenimine) revealed the existence of the hemihydrate, $(-\text{CH}_2\text{CH}_2\text{NH}-0.5\text{H}_2\text{O})_n$, besides the sesquihydrate and the dihydrate. It is therefore asserted that the anhydrate transforms into the hemihydrate, subsequently the sesquihydrate, and finally the dihydrate with increasing water content. The hemihydrate crystals are monoclinic, with cell dimensions $a = 1.089 \text{ nm}$, $b = 0.952 \text{ nm}$, c (fiber axis) $= 0.731 \text{ nm}$, and $\beta = 127.6^\circ$. The space group is $C2/c$, and the unit cell contains eight monomeric units (four chains) and four water molecules. The polymer chains are fully extended as in both the sesquihydrate and the dihydrate. All hydrogen bonds in the hemihydrate are of the $\text{N}-\text{H}\cdots\text{O}$ or $\text{N}\cdots\text{H}-\text{O}$ type: there exists no water-water hydrogen bond network, in contrast to the other two hydrates. The modes of hydrogen bondings in the anhydrate and the three hydrates are summarized and discussed. A variety of X-ray diffraction curves of poly(ethylenimine) are also presented for the use of identification of the crystal form (or forms) of a sample in question.

Previous X-ray studies¹⁻³ on linear poly(ethylenimine) (PEI) have revealed that the hygroscopic feature of this polymer is attributable to the formation of crystalline hydrates in which "water of crystallization" exists stoichiometrically. In practice, the PEI dihydrate contains a large quantity of water almost comparable to the weight of PEI itself. According to those studies, the polymer

chains take the fully extended form in the sesquihydrate and the dihydrate,¹ while the double-stranded helical form in the anhydrate.³ The striking difference in chain conformation between the anhydrate and the hydrates is the consequence of the full performance of hydrogen bondings in each crystal form; i.e., in all of the crystalline phases, every NH group and water molecule participate in hy-

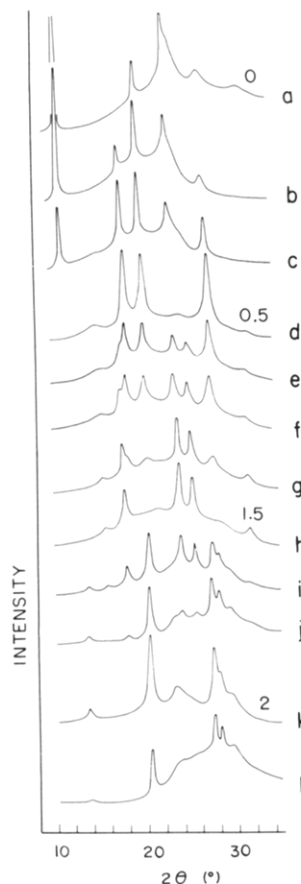


Figure 1. X-ray diffraction curves of PEI. Numbers 0, 0.5, and so on indicate the anhydrate, the hemihydrate, and so on.

drogen bondings. Besides these three crystalline phases, however, another crystalline phase has been found in the course of preparation of the anhydrate.³ Therefore, it is necessary to examine the structural change of PEI on hydration or dehydration in more detail. This paper will present that PEI can exist as four crystalline phases, depending on the water content, and the fourth crystalline phase newly found is the hemihydrate, $(-\text{CH}_2\text{CH}_2\text{NH}-0.5\text{H}_2\text{O})_n$. Structural characterization of the whole crystalline phase will be also summarized and discussed.

Experimental Section

We have reported^{1,2} that when the PEI anhydrate absorbs water vapor in air, the X-ray diffraction pattern changes progressively, depending on the temperature and the humidity (PEI exists preferentially as the sesquihydrate at room temperature in air). In order to examine the structural change on hydration or dehydration in more detail, X-ray diffraction curves for various PEI samples prepared under different physical conditions were taken with a Rigaku Denki diffractometer. The anhydrate sample was obtained from the melt,³ and the dihydrate sample was obtained by storing the sesquihydrate sample in a vessel of relative humidity of 100% at 35 °C for more than 1 day. Hydration of the anhydrate was carried out at several temperatures, 15, 20, 30, and 35 °C, under a relative humidity of 50 or 100% for a specified number of hours. Dehydration of the dihydrate was carried out by storing it in a desiccator at 15 or 20 °C. Many examples of the X-ray diffraction curves thus obtained are shown in Figure 1, in which the water content increases from the top trace to the bottom trace. As shown later, curve d is for the newly found hemihydrate. The water content of each sample was estimated by elemental analysis.

An oriented sample of the hemihydrate was prepared as follows. PEI powder was melted, dehydrated at 100 °C, and quenched in liquid nitrogen followed by stretching about five times. The oriented sample of 0.3-mm diameter was stored in a vessel of relative humidity about 50% at 15 °C for 1 day and then sealed off in a thin-walled Lindemann glass capillary. The sample was

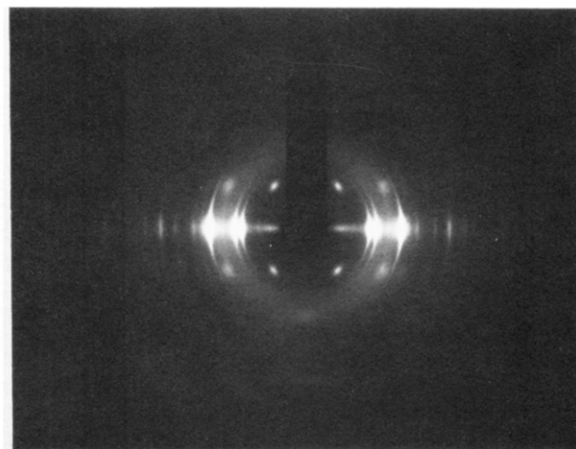


Figure 2. X-ray fiber photograph of the PEI hemihydrate.

checked by X-ray diffraction in order to confirm that the sample was free from other crystal forms. The X-ray fiber photograph of the hemihydrate is shown in Figure 2. The d spacings of reflections were obtained with a cylindrical camera of 45-mm radius and they were calibrated with aluminum powder. Reflection intensities were obtained by the multiple-film method and estimated visually. They were corrected for the Lorentz-polarization factor. X-ray diffraction curves of the hemihydrate (for example, curve d in Figure 1) were also used to estimate the intensity ratios among the layer lines of the fiber diagram. Fifty reflections were available.

Analytical Section

Variation of X-ray Diffraction Pattern on Hydration or Dehydration. Figure 1 shows the variation of the X-ray diffraction curve of PEI on hydration. The hydration of the anhydrate and the dehydration of the dihydrate exhibited reversely the same phase changes. We found a new crystalline phase (curve d in Figure 1) besides the anhydrate, the sesquihydrate, and the dihydrate reported so far. This new crystalline phase is the hemihydrate as will be shown later. The range between the hemihydrate and the sesquihydrate was studied in detail in order to reveal whether the monohydrate exists or not; in this range, however, each diffraction curve (curves e–g) is explained in terms of a mixture of the hemihydrate and the sesquihydrate with a certain mixing ratio. Gembitskii et al.⁴ reported that the hydration of PEI gave a crystalline X-ray diffraction pattern in which intense reflections were at $2\theta = 17.5, 23.5$, and 25.2° . Although they assigned the crystalline phase to the monohydrate, we suppose that the crystalline phase found by them is the sesquihydrate ($2\theta = 17.9, 24.0$, and 25.4° in our data for the sesquihydrate).

In addition, in order to examine whether another hydrate containing more water than the dihydrate exists, the X-ray diffraction curve (curve l in Figure 1) of a sample prepared by immersion of the dihydrate sample into hot water (45 °C) is shown; only the dihydrate is observed for this sample except strong X-ray scattering by water. From the observation shown in Figure 1, we would be able to conclude that there are no other crystalline phases than the four phases mentioned above.

The X-ray diffraction curves shown in Figure 1 will be available for identification of the crystal form (or forms) of a PEI sample in question. However, care must be taken to identify the crystal form of an unoriented sample. For example, curve e in Figure 1, which is for a mixture of the hemihydrate and the sesquihydrate, is very similar to curve i, which is for a mixture of the sesquihydrate and the dihydrate. In fact, we have hitherto been confused by this feature² and have failed to notice the existence of the hemihydrate.

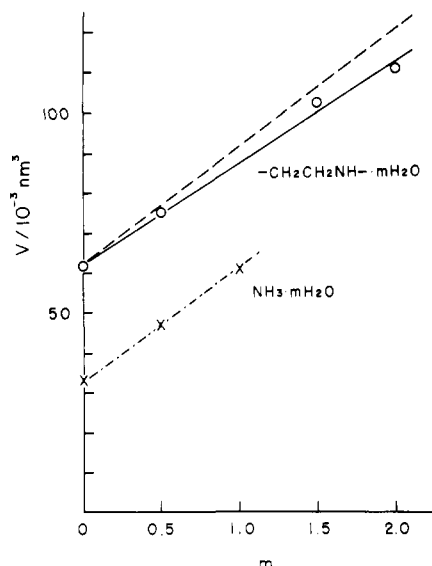


Figure 3. Plot of V vs. m for the PEI hydrates and the ammonia hydrates, where m is the hydration number and V means the volume of $-\text{CH}_2\text{CH}_2\text{NH}-m\text{H}_2\text{O}$ or $\text{NH}_3 \cdot m\text{H}_2\text{O}$.

Crystal Structure of the Hemihydrate. From the experimental fact mentioned above, the newly found crystalline phase must contain a smaller quantity of water than the sesquihydrate. Although elemental analysis of such crystalline polymer hydrates may bring about some extent of error to the conclusion because of the change of the weight during weighing by absorption or desorption of water and because of the existence of an amorphous region, which would exhibit a different behavior in absorption of water, the found chemical formula $\text{C}_2\text{H}_{5.7}\text{N}_{0.93}\text{O}_{0.48}$ seems to indicate that the new crystalline phase is the hemihydrate, $\text{C}_2\text{H}_5\text{N} \cdot 0.5\text{H}_2\text{O}$.

Two monoclinic unit cells that are different just in angle β explain well the observed d spacings (observed and calculated d spacings are listed in Table II): they are (unit cell A) $a = 1.089$ nm, $b = 0.952$ nm, c (fiber axis) = 0.731 nm, and $\beta = 127.6^\circ$ and (unit cell B) $a = 1.170$ nm, $b = 0.952$ nm, c (fiber axis) = 0.731 nm, and $\beta = 132.5^\circ$. Because the values of $a \sin \beta$ of both cells are equal, both cells have equal volume. For both cells, if the unit cell contains eight monomeric units and four water molecules as the hemihydrate, the calculated density is $1.15 \text{ g} \cdot \text{cm}^{-3}$, and this value is comparable to the observed density, $1.14 \text{ g} \cdot \text{cm}^{-3}$.

Figure 3 shows a plot of V vs. m , where m is the hydration number and V means the volume of $-\text{CH}_2\text{CH}_2\text{NH}-m\text{H}_2\text{O}$, which is calculated by the relation

$$V = abc \sin \beta / N$$

where N is the number of monomeric units per unit cell. The relation between V and m is fairly linear (the full line in Figure 3), and the slope of this line gives $25.5 \times 10^{-3} \text{ nm}^3 \cdot (\text{water molecule})^{-1}$, which can be regarded as the space occupied by one water molecule in the PEI hydrates. In Figure 3, the broken line is drawn under the assumption that V is expressed in terms of addition of the volume of the monomeric unit and of free water molecules, $29.9 \times 10^{-3} \text{ nm}^3 \cdot (\text{water molecule})^{-1}$. The observed value, $25.5 \times 10^{-3} \text{ nm}^3 \cdot (\text{water molecule})^{-1}$, is comparable to the values ($23\text{--}27 \times 10^{-3} \text{ nm}^3 \cdot (\text{water molecule})^{-1}$) for many hydrates of low molecular weight compounds. The half-dotted line in Figure 3 indicates similarly the relation between V and m for the ammonia hydrates, $\text{NH}_3 \cdot m\text{H}_2\text{O}$, for comparison.^{5,6} The linear relationship between V and m for PEI is therefore again an indication that the new crystalline phase is the hemihydrate.

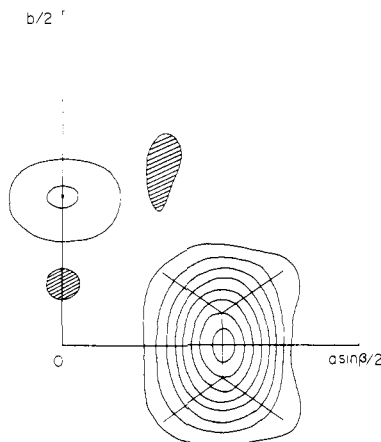


Figure 4. Electron density projected down the c axis. Contours are drawn at intervals of $2 \times 10^2 \text{ e} \cdot \text{nm}^{-2}$ starting at $2 \times 10^2 \text{ e} \cdot \text{nm}^{-2}$. Hatched areas are negative regions.

Although unit cells A and B give different Miller indices for each reflection of the layer lines ($h_A + h_B = -2l_A = -2l_B$, $k_A = k_B$, and $l_A = l_B$), systematic absences of the reflections that are common to both cells (hkl , $h + k = 2n + 1$; $h0l$, $h = 2n + 1$ and $l = 2n + 1$; $0k0$, $k = 2n + 1$) indicate that the space group of the hemihydrate is either Cc or $C2/c$, and the structure was explained by space group $C2/c$ as will be shown later.

The observed fiber period, 0.731 nm, together with the comparatively strong third layer line, establishes that the polymer chains are planar zigzag as in the sesquihydrate and the dihydrate; it means that four polymer chains pass through the unit cell. First, the structure of the ab projection, which is identical for both cells, was solved by trial and error. The intensities of the $hk0$ reflections with even h 's and k 's are generally strong, and they were roughly explained when the four polymer chains, whose main-chain plane is parallel to the bc plane, are located near ($x = 0.25$, $y = 0$), ($x = 0.75$, $y = 0$), and two other sites related to them by the symmetry of the C center. Since eight monomeric units contained in the unit cell can be located equivalently in the $C2/c$ lattice, space group $C2/c$ seemed to be preferred to Cc and was first assumed. The reflections with odd h 's and k 's are generally weak and they were explained when water molecules are introduced. In the $C2/c$ lattice, four water molecules can be disposed equivalently on the twofold rotation axes parallel to the b axis. In practice, all $hk0$ reflections were explained well by the $C2/c$ lattice. In the case of the Cc lattice, there are two kinds of monomeric units, but according to this space group, no other reasonable molecular packing was obtained. Since most of the $hk0$ reflections were individually observed, an $hk0$ Fourier synthesis was carried out. Figure 4 illustrates the final electron density map of the ab projection.

The three-dimensional structure was then solved by shifting the polymer chains along the c axis for both cells. The height of the polymer chain was uniquely determined for both cells, giving very similar structures except the difference in angle β . Since many diffraction spots of the layer lines consist of several hkl reflections overlapped, the three-dimensional Fourier synthesis could not be applied. The structures for both cells were then refined by the diagonal least-squares method, in which the quantity $\sum (I_o^{1/2} - I_c^{1/2})^2$ was to be minimized, where $I = \sum m F^2$ (F is the structure factor, m is the multiplicity of reflection, and summation is made for overlapped reflections). The difference in angle β of both unit cells affects particularly reflection intensities of the third layer line: unit cell B gives rather poor agreement between observed and calcu-

Table I
Atomic Coordinates, Thermal Parameters, and Their
Estimated Standard Deviations

atom	x	y	z	$B/10^{-2}$ nm ²
C(1)	0.235 (4)	0.550 (4)	0.360 (8)	6.6 (1.3)
C(2)	0.231 (4)	0.550 (4)	0.694 (8)	6.7 (1.3)
N	0.233 (3)	0.458 (3)	0.527 (6)	6.6 (1.0)
O	0.500	0.278 (4)	0.750	6.6 (1.1)

lated intensities and also gives unreasonable bond lengths by this refinement. The reliability factor ($R = \sum |I_o^{1/2} - I_c^{1/2}| / \sum I_o^{1/2}$) for the third layer line is 0.14 for unit cell A, but 0.32 for unit cell B, and for all observed reflections, the R factor is 0.14 for unit cell A and 0.19 for unit cell B. Besides, several nonobserved reflections of the third layer line have large calculated intensities for unit cell B but not for unit cell A. Therefore unit cell A should be

adopted. The CH₂ hydrogen atoms were included in the calculation of intensities assuming a C-H bond length of 0.109 nm and a H-C-H bond angle of 109.5°, but the hydrogen atoms of NH group and of water were ignored as will be discussed later. The final atomic coordinates and thermal parameters are shown in Table I. The observed and calculated structure factors are listed in Table II.

Results and Discussion

Molecular Structure in the Hemihydrate. The polymer chains in the hemihydrate are essentially planar zigzag as in the sesquihydrate and the dihydrate: the deviations of the x coordinates of the main-chain atoms from the planar-zigzag form are within the estimated standard deviation of the x coordinates, 0.004. Bond lengths and bond angles obtained from the atomic coordinates shown in Table I are as follows: C-C, 0.154 nm; C-N, 0.150 nm; C-C-N, 104°; C-N-C, 109°.

Table II
Observed and Calculated Spacings and Structure Factors of the PEI Hemihydrate

$h k l$	d_o/nm	d_c/nm	$(mF_o^2)^{1/2}$	$(mF_c^2)^{1/2}$	$h k l$	d_o/nm	d_c/nm	$(mF_o^2)^{1/2}$	$(mF_c^2)^{1/2}$
1 1 0	0.640	0.639	11	12	-5 1 2	0.210	0.212	11	6
0 2 0	0.478	0.476	92	77	-2 4 2	0.197	0.199	13	14
2 0 0	0.429	0.431	95	89	2 0 2	0.189	0.192	13	14
2 2 0	0.321	0.320	124	135	1 3 2		0.189		
1 3 0	0.297	0.298	17	23	0 4 2		0.184		2
3 1 0	0.276	0.275	38	40	-6 0 2		0.180		
0 4 0	0.238	0.238	27	25	-5 3 2	0.177	0.179	14	12
4 0 0		0.216			2 2 2		0.178		
3 3 0	0.215	0.213	49	62	-4 4 2		0.178		
2 4 0	0.208	0.208	14	10	-6 2 2		0.168		
4 2 0	0.198	0.196	30	36	-1 5 2	0.167	0.167	15	11
1 5 0	0.186	0.186	13	13	-3 5 2		0.165		
5 1 0	0.169	0.170	15	23	3 1 2		0.158		1
4 4 0		0.160			-7 1 2		0.150		
0 6 0	0.159	0.159	30	33	2 4 2	0.148	0.149	14	10
3 5 0		0.159			1 5 2		0.148		
5 3 0	0.153	0.152	16	19	-2 6 2		0.145		1
2 6 0		0.149		6	3 3 2		0.143		
6 0 0	0.144	0.144	15	14	-6 4 2	0.142	0.143	12	10
6 2 0	0.138	0.138	27	30	-5 5 2		0.143		
1 7 0	0.133	0.134	10	6	-1 1 3	0.214	0.213	35	29
4 6 0		0.128			-2 2 3		0.213		
5 5 0	0.127	0.128	10	10	-4 2 3	0.207	0.206	26	19
6 4 0		0.123			-5 1 3		0.200		7
3 7 0	0.123	0.123	17	19	-3 3 3	0.192	0.193	25	13
7 1 0		0.122			-1 3 3	0.181	0.180	44	42
-1 1 1	0.581	0.578	29	21	0 2 3	0.171	0.179	21	22
0 2 1		0.368		7	-5 3 3		0.172		
-2 2 1		0.356			-2 4 3		0.168		
1 1 1	0.355	0.356	27	27	-6 2 3	0.165	0.167	49	49
-3 1 1	0.334	0.336	21	17	1 1 3		0.165		
-1 3 1	0.292	0.291	22	19	-4 4 3		0.165		
1 3 1	0.245	0.245	15	14	-7 1 3		0.153		11
-3 3 1		0.238			-3 5 3		0.150		
2 2 1	0.238	0.238	18	21	0 4 3	0.148	0.150	37	35
-4 2 1		0.229		8	1 3 3		0.148		
0 4 1		0.220			-1 5 3	0.143	0.144	30	25
-2 4 1	0.218	0.218	21	15	-6 4 3		0.143		
3 1 1	0.206	0.206	13	14	2 2 3		0.139		
-5 1 1	0.198	0.198	14	16	-5 5 3		0.139		11
-1 5 1	0.186	0.184	15	12	-2 6 3		0.132		
-1 1 2		0.324		4	-8 2 3	0.132	0.131	28	24
-3 1 2		0.309		3	-4 6 3		0.130		
0 0 2		0.289			3 1 3	0.126	0.127	23	19
-2 2 2	0.290	0.289	18	20	1 5 3		0.126		
-4 0 2	0.266	0.268	10	9	2 4 3		0.124		
0 2 2	0.248	0.247	20	21	0 6 3		0.123		4
-4 2 2		0.234			-7 5 3		0.120		
-1 3 2		0.233			3 3 3		0.119		
-3 3 2	0.232	0.228	18	22	-3 7 3	0.119	0.119	34	30
1 1 2		0.228			-6 6 3		0.119		
					-9 1 3		0.119		
					-8 4 3		0.118		

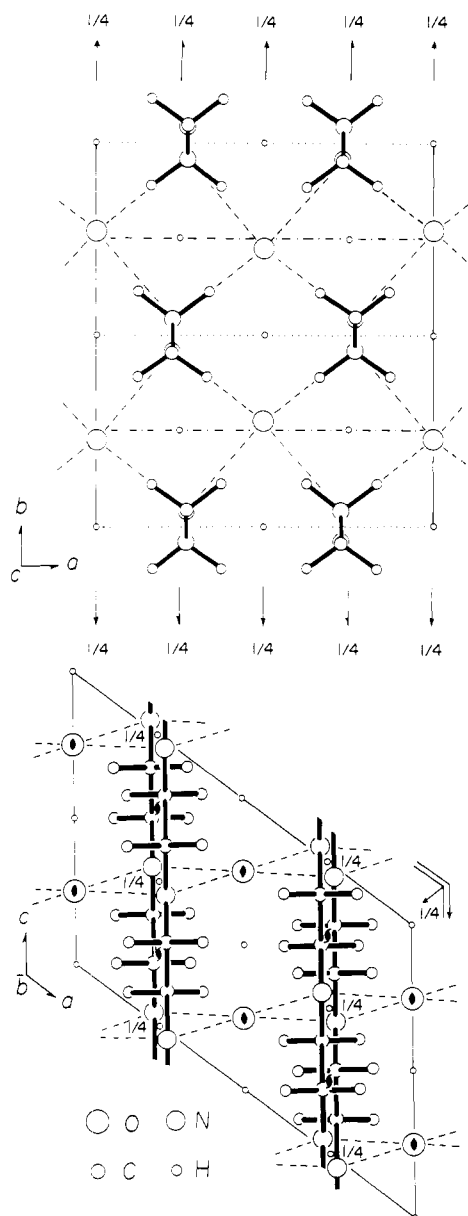


Figure 5. Crystal structure of the PEI hemihydrate. Broken lines indicate hydrogen bonds, but hydrogen atoms of NH groups and of water molecules are omitted.

Table III
Dimensions of Hydrogen Bonds in the PEI Hemihydrate

Distances, nm			
$N(A) \cdots O(w)$	0.305	$N(A') \cdots O(w)$	0.287
Angles, deg			
$N(A) \cdots O(w) \cdots N(A')$	85.3	$N(B) \cdots O(w) \cdots N(B')$	85.3
$N(A) \cdots O(w) \cdots N(B)$	85.2	$N(A') \cdots O(w) \cdots N(B')$	106.8
$N(A) \cdots O(w) \cdots N(B')$	164.0	$N(A') \cdots O(w) \cdots N(B)$	164.0

Crystal Structure of the Hemihydrate. The packing of the polymer chains and the water molecules in the hemihydrate is shown in Figure 5. The mode of molecular packing is rather similar to that of the sesquihydrate. The main-chain planes are parallel to the *bc* plane, and the water oxygen atoms are on the twofold rotation axes parallel to the *b* axis. In Figure 5, broken lines indicate $N \cdots H \cdots O$ or $N \cdots H \cdots O$ hydrogen bonds, and Table III summarizes the $N \cdots O$ distances and the coordination angles at the water oxygen atom.

As for the coordination about water molecules in various hydrates of low molecular weight compounds containing

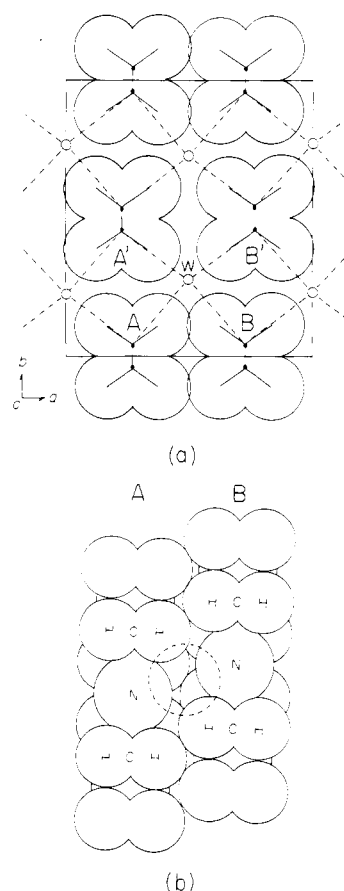


Figure 6. (a) Schematic end view of the PEI hemihydrate and (b) the space-filling side view of the two chains separated by 0.400 nm. Broken circle represents a water oxygen atom.

water and nitrogen atoms, the water oxygen atoms are tetrahedrally coordinated by water oxygen atoms or nitrogen atoms. The coordination angles at the water oxygen atoms in the PEI sesquihydrate and dihydrate are indeed close to the tetrahedral value: the mean value of the coordination angles and the standard deviation are 108 and 11° , respectively, for the sesquihydrate and 108 and 12° for the dihydrate (cf. 108.7 and 14.7° for various hydrates of low molecular weight compounds⁷). In the PEI hemihydrate, however, some anomalies arise in the coordination angles as shown in Table III: the plane $N(A)O(w)N(B)$ makes an angle of 21° to the plane $N(A')O(w)N(B')$ (the angle should be 90° for regular tetrahedral coordination). The mean value of the coordination angles and the standard deviation are thus 115 and 35° , respectively, for the hemihydrate. Potassium oxalate monohydrate is known to exhibit an exceptionally unusual coordination; i.e., the water molecule takes an approximately planar coordination of four nearest neighbors, two potassium ions and two oxalate oxygen atoms.^{8,9} We therefore need to examine why such an unusual coordination is taken in the PEI hemihydrate. There are two kinds of nonequivalent $N \cdots O$ pairs, and their distances are different from each other. The $N(A') \cdots O(w)$ distance is short, 0.287 nm. This close approach can be achieved because there is no steric hindrance between polymer chains A' and B' (Figure 6a). On the other hand, the $N(A) \cdots O(w)$ distance is rather long, 0.305 nm. As seen in the end view of Figure 6a, in this case the van der Waals shells of the CH_2 groups of polymer chains A and B are overlapped; then the relative shift of the two chains along the chain axis prevents the steric hindrance (Figure 6b). Therefore, it seems that the unusual coordination is the consequence of a balance between

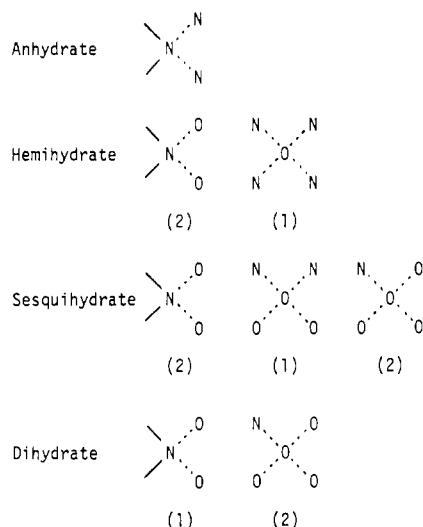
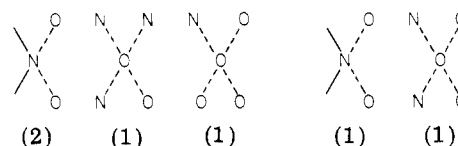


Figure 7. Coordination schemes of hydrogen bondings in the PEI anhydrate and the three hydrates. Numbers in parentheses indicate relative proportions of appearance.

the stability of the tetrahedral coordination and the prevention of the steric hindrance between the polymer chains of the planar-zigzag conformation. It is well-known that $X-H\cdots Y$ hydrogen bonds are allowed to bend to some extent: in various hydrates the bend angle, defined as the angle between $X-H$ and $H\cdots Y$, is in the range between 20 and 25°. Since NH nitrogen atoms of PEI take the pyramidal structure like ammonia,¹ it is reasonable that some appropriate orientations of the water molecules enable the NH groups and the water molecules to form $N-H\cdots O$ and $N\cdots H-O$ hydrogen bondings. Again, it seems that the short hydrogen bonds, 0.287 nm, are of the $N\cdots H-O$ type and the long ones, 0.305 nm, are of the $N-H\cdots O$ type (in the ammonia hemihydrate and monohydrate, hydrogen bonds longer than 0.313 nm were assigned to the $N-H\cdots O$ type, and hydrogen bonds shorter than 0.285 nm to the $N\cdots H-O$ type). As for all of the PEI crystalline forms, however, the positions and the behaviors of hydrogen atoms of water molecules and of NH groups, which are closely related to "nitrogen inversion", are unresolved and interesting problems.

Hydrogen Bondings in Four PEI Crystalline Forms. Evidently hydrogen bondings play the major role in the formation of the four kinds of PEI crystals. Figure 7 summarizes the hydrogen-bonding schemes in the four crystalline phases; here, the hydrogen atoms of the NH groups and of the water molecules are omitted. In the anhydrate, each nitrogen atom is coordinated by two NH groups (and two CH_2 groups). In all of the hydrates, every nitrogen atom is coordinated by two water molecules instead of two NH groups; it should be noted that in both ammonia hemihydrate and ammonia monohydrate, every nitrogen atom is again coordinated by water molecules only. As for the water molecules in the PEI hydrates, three kinds of coordination schemes are found. In the hemihydrate, each oxygen atom is coordinated by four NH groups. In the sesquihydrate, there are two kinds of water molecules: one is coordinated by two NH groups and two water molecules, and the other is coordinated by one NH group and three water molecules, the proportion of the former and the latter being 1:2. In the dihydrate, each oxygen atom is coordinated by one NH group and three water molecules. In any event, these coordinations enable all of the NH groups and water molecules to participate in hydrogen bondings.

Besides, if PEI can exist as the monohydrate, the plausible coordination scheme is either of the following two cases:



Here, numbers in parentheses imply the proportions as stated in Figure 7. However, no PEI monohydrate has been found. From the viewpoint of stereochemistry, both schemes appear to be unfavorable to build up a three-dimensional crystal lattice, even through these coordinations might be realized as local structures in the amorphous region.

As previously reported,¹ water molecules themselves create a network connected by $O-H\cdots O$ hydrogen bonds in the sesquihydrate and the dihydrate (more precisely, a ribbon structure in the sesquihydrate and a sheet structure in the dihydrate). The structural unit of the water network in the dihydrate (six-oxygen-atom ring) is the same as that in ordinary ice, while the structural unit in the sesquihydrate (five-oxygen-atom ring) is basically the same as one of the structural units that construct water polyhedra in gas hydrates and in other modifications of ice. In contrast, the water molecules in the hemihydrate are too far apart to create any water network.

Conclusion

PEI exists as the hemihydrate under relatively low water vapor pressures, in which the polymer chains are planar zigzag and all of the hydrogen bonds are of the $N-H\cdots O$ or $N\cdots H-O$ type. We have found no crystalline hydrate of smaller water content than the hemihydrate or of larger water content than the dihydrate. We believe that the hemihydrate is the crystalline phase of the smallest stoichiometric water content in which all of the NH groups and water molecules are able to participate in hydrogen bondings. It can therefore be asserted that the anhydrate transforms into the hemihydrate, subsequently the sesquihydrate, and finally the dihydrate with increasing water content. In any event, the conformation of the PEI chains change drastically from the double-stranded helical form in the anhydrate to the fully extended form in the hydrates. The thermodynamic stabilities and properties of the four crystal forms are, however, not yet certain and are now under study.

Acknowledgment. We express our sincere thanks to Prof. T. Saegusa of Kyoto University and Dr. R. Tanaka of Kyushu University for supplying PEI samples.

Registry No. PEI, 9002-98-6.

References and Notes

- Chatani, Y.; Tadokoro, H.; Saegusa, T.; Ikeda, H. *Macromolecules* **1981**, *14*, 315.
- Chatani, Y. Abstracts of U.S.-Japan Polymer Symposium, Palm Springs, 1980. *Contemp. Top. Polym. Sci.*, in press.
- Chatani, Y.; Kobatake, T.; Tadokoro, H.; Tanaka, R. *Macromolecules* **1982**, *15*, 170.
- Gembitskii, P. A.; Kleshcheva, N. A.; Golitsyna, T. L.; Nikolaev, G. M.; Zhuk, D. S. *Izv. Akad. Nauk SSSR, Ser. Khim.* **1975**, *11*, 2622.
- Siemons, W. J.; Templeton, D. H. *Acta Crystallogr.* **1954**, *7*, 194.
- Olovsson, I.; Templeton, D. H. *Acta Crystallogr.* **1955**, *12*, 827.
- Franks, F., Ed. "Water"; Plenum Press: New York, London, 1973; Vol. 2.
- Chidambaram, R.; Sequeira, A.; Sikka, S. K. *J. Chem. Phys.* **1964**, *41*, 3616.
- Pederson, B. F. *Acta Chem. Scand.* **1964**, *18*, 1635.